ACS APPLIED MATERIALS & INTERFACES

Research Article

www.acsami.org

# Hydrogen Evolution Using Palladium Sulfide (PdS) Nanocorals as Photoanodes in Aqueous Solution

M. Barawi, I. J. Ferrer,* J. R. Ares, and C. Sánchez

Materials of Interest in Renewable Energies Laboratory (MIRE), Departmento de Física de Materiales, Universidad Autónoma de Madrid, Madrid 28049, Spain

Supporting Information

**ABSTRACT:** Palladium sulfide (PdS) nanostructures are proposed to be used as photoanodes in photoelectrochemical cells (PECs) for hydrogen evolution due to their adequate transport and optical properties shown in previous works. Here, a complete morphological and electrochemical characterization of PdS films has been performed by different techniques. PdS flatband potential (Vfb = −0.65 ± 0.05 V vs NHE) was determined by electrochemical impedance spectroscopy measurements in aqueous $Na_2SO_3$ electrolyte, providing a description of the energy levels scheme at the electrolyte−semiconductor interface. This energy levels scheme confirms PdS as a compound able to photogenerate hydrogen in a PEC. At last, photogenerated hydrogen rates are measured continuously by mass spectrometry as a function of the external bias potential under illumination, reaching values up to 4.4 $\mu$mol$H_2$/h at 0.3 V vs Ag/AgCl.

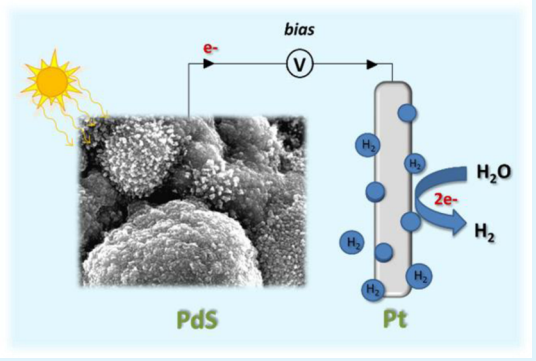


**KEYWORDS:** *hydrogen generation, photoelectrochemistry, energy photoconversion, palladium sulfide, solar energy conversion*

## INTRODUCTION

Interest in hydrogen generation from water by solar radiation is motivated by the need to find a green, renewable and environmentally safe fuel. Hydrogen is considered as a viable option to bring the energy mix toward a cleaner and more sustainable alternative, especially when it is produced from water by using only renewable energy sources. In addition, production of fuels would provide a globally scalable solution to the storage problem associated with the regional intermittency of renewable energies. To this aim, the use of solar energy as a renewable source is a very attractive and appropriate option.[1,2]

Since Honda and Fujishima discovered in 1972 the possibility to produce hydrogen in a photoelectrochemical cell (PEC),[3] many scientists have shown interest in finding suitable materials for hydrogen generation using solar energy by this method. The main characteristics required by a semiconducting photoelectrode to be used in a successful PEC for solar water splitting include, having appropriate band gap energy (at least 1.6−1.7 eV and less than 2.3−2.4 eV), high stability in aqueous solutions and a suitable position of the energy band edges versus water redox potentials.[4] However, most of materials investigated (metal oxides)[5] only work under ultraviolet light (UV) and/or exhibit low activity under visible light, which is a big drawback because the majority of radiation on the earth is composed of visible light.

Metal sulfides for solar water splitting have been chosen because of their low cost, abundance, easy manufacture and adequate transport properties (mainly low electrical resistivity). In addition, some metal sulfides exhibit appropriate optical properties (mainly, but not only, band gap energy) to be used as photoanode for hydrogen generation. Cadmium sulfide (CdS) is the most extensively metal sulfide studied since the 1970s,[6,7] but its toxic behavior means that other binary sulfides have also been investigated ($RuS_2$, CdSe, CoS, $MoSe_2$, ...).[8,9]

Palladium sulfide (PdS) is proposed for this goal due to its high potential for photocatalysis applications, i.e., its optical absorption coefficient (higher than $10^5$ $cm^{-1}$ at photon energies $h\nu$ > 2.0 eV)[10] and its adequate band gap energy, which has been reported in the range of 1.6−2.0 eV.[10−13] All these properties make PdS attractive for photoelectrochemical hydrogen generation. However, reports on the photoelectrochemical properties of PdS are scarce. The first results, proceeding from *n*-type PdS crystals, reported by Folmer et al.,[12] showed very low photoresponse and a band gap energy of 2.14 eV. Nevertheless, these results were not very confident due to the low values of the photocurrents. Preliminary studies of the photoelectrochemical properties of PdS, performed in our group, confirms the photoactivity of PdS in aqueous solutions of $Na_2SO_3$ at bias potential higher than 200 mV (Ag/AgCl)[13] and a band gap energy of about 1.8 eV, according with that optically determined.[10] Recently, PdS has also been investigated as a photocatalyst for photocatalytic hydrogen production beside other sulfides, mainly CdS.[14−17] In those reports, it has been demonstrated that the presence of PdS alone and with Pt and other noble metals as Au, Rh, Ru, enhanced the rate of hydrogen photogeneration.

Received: September 11, 2014
Accepted: October 23, 2014
Published: October 23, 2014

  

In this work, the suitability of PdS to be used in a PEC is evaluated, by means of flat band potential determination in order to establish the energy levels scheme for the electrolyte/PdS interface. In addition, its utilization as a photoanode in a photoelectrochemical cell for hydrogen production has been investigated. Finally, the rate of hydrogen evolution has been measured, whose values are comparable to those obtained with more complicated photoelectrode structures.[18] Finally, the photoconversion efficiency has been estimated.

## EXPERIMENTAL SECTION

**Synthesis of PdS Nanocorals.** To get palladium sulfide (PdS) nanostructures, palladium thin films have been deposited on titanium discs (Goodfellow 99.9%, Ø = 10 mm). Palladium (Goodfelow 99.95%) was evaporated in an electron gun (mod. Telstar) at room temperature, under a residual vacuum pressure of $10^{-7}$ mbar (5 kV, ~50−100 mA). In situ film thickness (100 ± 10 nm) was measured by a piezoelectric crystal available in the evaporation chamber. Afterward, sulfuration of Pd films was carried out in vacuum sealed ampules with sulfur powder (Merck, 99.75%) at 350 °C for 20 h.

**Structural and Morphological Characterization.** X-ray diffraction (XRD) patterns were carried out with an X'Pert PRO Panalytical diffractometer in order to identify the crystalline phases and analyze their structure. Crystallite size was calculated using the Scherrer equation.[19] Images from field emission microscopy (FEG, model FEI XL-30) and Atomic Force Microscopy (AFM, Dulcinea and Cervantes system) were used to characterize the film morphology. Finally, the chemical composition of films was determined by energy dispersive X-ray analysis (EDX, model INCA x-sight).

**Electrochemistry.** Electro- and photoelectrochemical measurements have been carried out by using a three-electrode glass cell with a quartz window to allow the photoanode illumination. PdS thin films were used as the working electrode. The counter electrode and reference were a platinum sheet and an Ag/AgCl reference electrode, respectively. A 0.5 M $Na_2SO_3$ aqueous solution was used as the electrolyte, which serves both to improve the conductivity and as a sacrificial agent. A 200 W halogen lamp was used as the illumination source. Measured light power density reaching the surface sample was 270 ± 20 mW/cm$^2$. This value was used to estimate the photoconversion efficiency of the system as indicated below.

Potentiodynamic electrochemical impedance spectroscopy (EIS)[20,21] was performed by using the AUTOLAB PGSTAT302N Potentiostat, provided with an integrated impedance module FRAII. The superimposed AC signal was maintained at 10 mV of wave amplitude while the frequency was scanned from 100 Hz to 1 kHz. Obtained data were then treated with the NOVA software. This technique provides information about the potential-dependence of semiconductor−electrolyte interface. To determine the flat band potential, capacitance from space charge layer was calculated from the imaginary part of the impedance. These data have been analyzed by the Mott−Schottky equation.[22]

**Hydrogen Evolution.** Hydrogen quantification was carried out by means of a mass spectrometer (QMS, model Prisma, Balzers) coupled to the sealed photoelectrochemical cell. During the experiment, an argon flow of 20 SSCM was passed through the top of the cell. Hydrogen calibration of the mass spectrometer was previously made by introducing a known flow of argon and hydrogen provided by a metal hydride bottle, designed in our laboratory, capable of storing 2 g of hydrogen (Supporting Information). The gases released during the photoelectrochemical reactions are quantified by photoelectrochemical mass spectrometry (PMS), i.e., a quadruple mass spectrometer (QMS) coupled to the PEC, which allows one to collect a high number of measurements in a very low timeframe (10 measures/min). In spite of gas chromatography (GC) being habitually used to identify the amount of species released during the photoelectrochemical reaction,[23,24] the PMS technique exhibits some advantages such as a high accuracy to detect light elements as hydrogen as well as provides isotopic information if needed.

In general, the overall photoconversion efficiency, $\eta(\%)$, is estimated by the following equation[25]

$$\eta = \frac{\Delta G^0_{H_2} R_{H_2} - V_b \cdot I}{P_S} \times 100 \quad (1)$$

Where $\Delta G^0_{H_2}$ ($\Delta G^0_{H_2}$ = 237.2 kJ/mol) is the standard Gibbs energy at 25 °C and 1 bar of water splitting, $R_{H_2}$ is the rate of production of hydrogen (mol/s), in its standard state per unit area of the photoelectrode, $P_S$ is the power density of illumination (W/m$^2$), $V_b$ is the external bias potential (V) and $I$ is the current density (A/m$^2$) responsible for the generation of hydrogen at the rate $R_{H2}$; therefore, it is assumed that all the carriers contribute to generating hydrogen. This equation is used when an external electrical bias is needed. The efficiency has been estimated by this equation.

## RESULTS AND DISCUSSION

**Photoelectrodes Synthesis and Characterization.** X-ray diffraction patterns of evaporated Pd films before and after sulfuration are shown in Figure 1. The Pd cubic structure

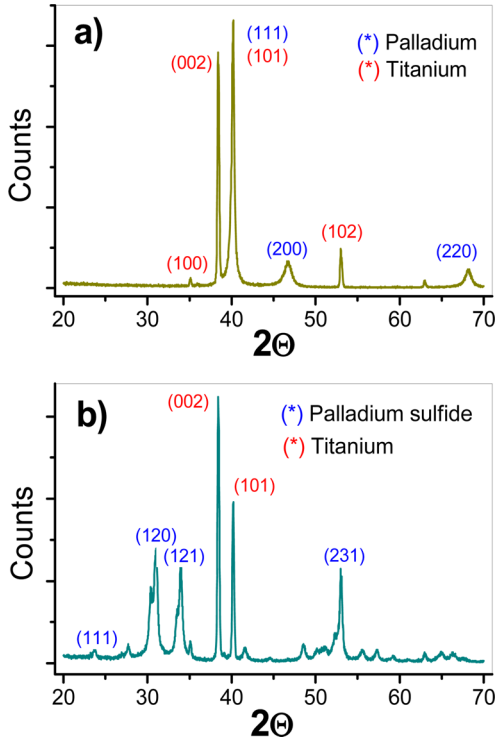


**Figure 1.** X-ray diffraction patterns of Pd (a) and PdS (b) thin film deposited on titanium.

(*Fm*3*m*) was identified according to JCPDS-ICDD 46-1043 from the pattern of Pd film (Figure 1a). The average crystallite size, estimated from the broadening of the (111) XRD peak, was 14 ± 2 nm and the lattice parameter $a$ = 3.900 ± 0.005 Å, which is slightly higher than the tabulated one ($a$ = 3.890).[26] Pd film electrical resistivity ($\rho$) and Seebeck coefficient ($S$), investigated in samples deposited on quartz, show values of 6 ± 1 × $10^{-5}$ Ω·cm and 5.9 ± 0.5 μV/K, respectively. These values are in agreement with those previously reported.[10] Figure 1b shows the XRD pattern obtained from a sulfurated Pd thin film in which the tetragonal PdS phase is identified according to JCPDS-ICDD 78-0206. The average crystallite size, estimated from the broadening of the (210) XRD peak is 30 ± 2 nm and the lattice parameters are $a$ = $b$ = 6.30 ± 0.01 Å and $c$ = 6.73 ±


dx.doi.org/10.1021/am5061504 | ACS Appl. Mater. Interfaces 2014, 6, 20544−20549

0.01 Å. These values hint a slightly compressed lattice in comparison with the reported values ($a = b = 6.429$ Å, $c = 6.611$ Å).[26] Stoichiometric ratio of S/Pd = 1.00 ± 0.05 was estimated by energy dispersive X-ray spectroscopy (EDX) confirming the presence of PdS.

Film thickness of Pd deposited on quartz grows during sulfuration, reaching 3.5 times the initial one due to the transformation on PdS.[10,27] According to this fact, the estimated PdS thickness is 350 nm, approximately. Direct thickness measurements by profilometry are no adequate due to the roughness of the titanium substrate.

FEG images of PdS films are shown in Figure 2 as a series of pictures. As can be appreciated, palladium sulfide comprises a

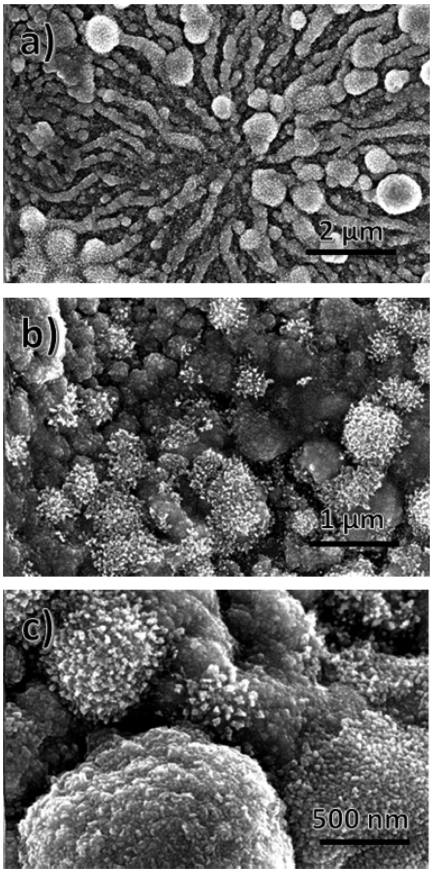


**Figure 2.** (a–c) Surface FEG images from PdS nanocorals at different magnifications.

quirky morphology very similar to that of corals in nature. This morphology seems to be formed by irregular spheres, which, in turn, are composed, as shown in the image of higher magnification, by submicrometer balls. This type of structure should facilitate the catalytic processes, because of the large surface roughness and, therefore, the high specific area which would result in a charge transfer processes more effective.

To investigate thoroughly the film morphology, and to know the real area of our photoelectrode, AFM microscopy has also been used. Images, shown in Figure 3, were taken with different augmentations. Details of these images have been treated with the software WSxM 5.0 Develop 6.4.[28] The total specific area has been obtained in a 1 $\mu m^2$ of sample resulting in $A_T = 1.5 \pm 0.1$ $\mu m^2$, i.e., is a 50% higher than the geometric one. Therefore, direct sulfuration provides an easier method to obtain wide surfaces compared to other synthesis more complicated as

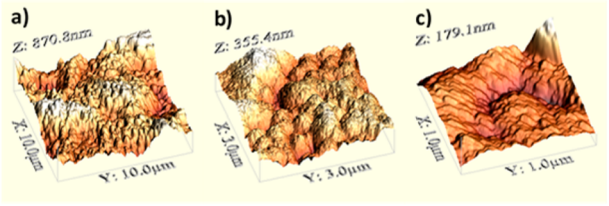


**Figure 3.** AFM images at (a) 10, (b) 4 and (c) 1 $\mu$m.

electrodeposition. This result hints that this morphology increases the area in contact with the electrolyte and, therefore, should improve the charge transfer at the interface.

Figure 4 shows a roughness analysis of the samples. In the profile drawn inset of Figure 4a, the magnitude of the roughness could be seen, showing that synthesized PdS has a high surface area. The topography analysis hints that PdS grains have different sizes but more than the 50% are between 300 and 600 nm. Because the average crystallite size, determined from XRD patterns, is 30 nm, these grains should be formed by 10–20 crystallites.

**Electrochemical Characterization and Flat Band Potential Determination.** Materials for water splitting in a photoelectrochemical cell have to fulfill several requirements.[29,30] The Gibbs free energy change for the conversion of one molecule of $H_2O$ to $H_2$ and $1/2O_2$ under standard conditions is $\Delta G = 237.2$ kJ/mol, which, according to Nernst equation, corresponds to $\Delta E^\circ = 1.23$ eV per electron transfer:[31]

$$H_2O \rightarrow \frac{1}{2}O_2 + H_2 \quad \Delta G = +237.2 \text{ KJ/mol}$$

Therefore, the semiconductor band gap energy ($E_g$) must be higher than 1.6–1.7 eV to overtake the minimum theoretical difference in the equilibrium potentials between the oxidation and reduction reactions (1.23 eV at 25 °C) and the overpotential needed to produce the water splitting.[25] Moreover, the semiconductor band gap energy should be less than 2.3–2.4 eV to absorb radiation in the range of solar visible light. In order to resume all of these requirements, they are exposed in Table 1.[32,33] Furthermore, semiconductor energy band edge position should straddle the water redox potentials. The edge of the valence band energy must be below the water oxidation potential to oxygen, as well as the lower edge of the conduction band energy must be above the water reduction potential of hydrogen.

PdS fulfills the band gap energy requirement because its $E_g$ is 1.6–1.8 eV, as determined from optical absorption[10,27] and photoelectrochemical measurements in previous works.[13] Then, in order to know the energy band edges position at the interface, the flat band potential, $V_{fb}$, should be determined. Flat band potential performs, in semiconductor electrochemistry, a role similar to that played by the zero charge potential in the metal–electrolyte interface.

Here, the $V_{fb}$ of PdS thin films has been obtained from space charge layer capacitance ($C_{SC}$) measured by potentiodynamic electrochemical impedance spectroscopy, EIS. To determine the space charge layer capacitance, AC modulated cyclic voltage scans from −1.5 V to +0.5 V in a range of frequencies between 100 Hz and 1 kHz, under dark conditions, were performed. The capacitance of the space charge layer is calculated by assuming

$$1/(wZ_{im}) = C_{SC} \quad (2)$$

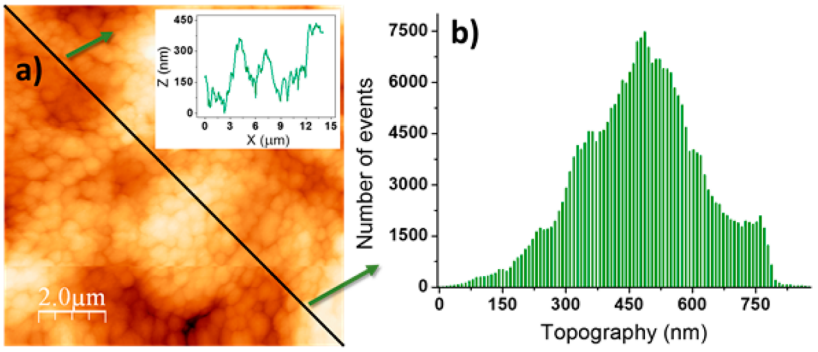


**Figure 4.** AFM roughness analysis: (a) image and profile (inset), (b) topography.

**Table 1. Main Requirements to $H_2$ Evolution by Means of Solar Water Photosplitting in Semiconductor–Liquid Junctions**

| conditions | main requirements |
|---|---|
| PEC water splitting | $H_2O(l) + 2h\nu \rightarrow 1/2O_2(g) + H_2(g)$ |
| minimum theoretical potential required | $E^\circ$ $H_2O$ (25 °C)$_{min}$ = 1.229 eV |
| practical potential (+overpotential and losses) | $E^\circ$ $H_2O$ (25 °C)$_{prac.}$ = 1.6–2.0 eV; $E_{gap} > E^\circ$ $H_2O$ |
| for efficient utilization of sunlight | 2.4 eV $\geq E_g \geq$ 1.7 eV; $h\nu \geq E_{gap}$ |
| band edges requirement | $E_{CB} < E^\circ$ $H_2/H^+$; $E_{BV} > E^\circ$ $O_2/H_2O$ |

The dependence of $C_{SC}$ on bias potential (V) is described by the Mott–Schottky eq 3:

$$\frac{1}{C_{SC}^{\ 2}} = \left(\frac{2}{\varepsilon_{SC}\varepsilon_0 N_D e_0}\right)\left([V - V_{fb}] - \frac{k_B T}{e_0}\right) \quad (3)$$

where $C_{SC}$ is the measured differential capacitance per area unit, $e_0$ is the elementary charge, $\varepsilon_{SC}$ is the PdS dielectric constant, $\varepsilon_0$ is the electrical permittivity of vacuum, $N_D$ is the semiconductor donor density, $V$ is the applied bias potential in volts, $k_B$ is Boltzmann's constant and $T$ is temperature (298 K). Therefore, from the $C_{SC}^{-2}$ vs $V$ plot, $V_{fb}$ can be easily obtained by the interception with the $x$-axis.[25]

Figure 5 shows the $C_{SC}^{-2}$ vs $V$ plots of a PdS film performed at different frequencies. All plots are straight lines that intercept

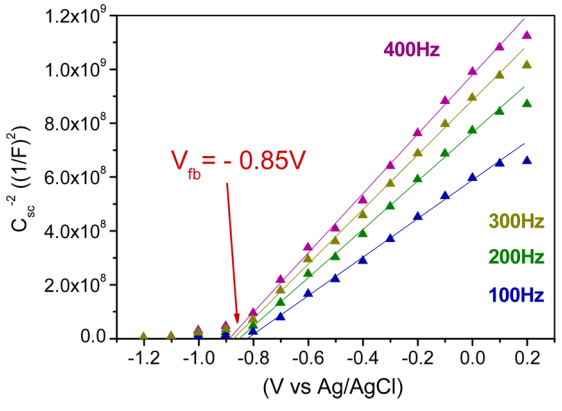


**Figure 5.** Mott–Schottky plots of a PdS thin film at different frequencies.

at $x$-axis position in the flat band potential of PdS giving $V_{fb}$ = −0.85 ± 0.05 V vs (Ag/AgCl), i.e., −0.65 V ± 0.05 V (NHE). This value is more positive than that reported by Folmer[12] (−1.3 to −1.6 V(SCE), i.e., −1.06 to −1.36 V (NHE)) and more negative than that reported by Yan[14] (−0.5 V(SCE), i.e., −0.26 V(NHE)) but those works do not show a detailed explanation of experimental conditions used (electrolyte, pH, frequency, etc.)

The value of $V_{fb}$ obtained here places the position of the PdS conduction band energy edge, depicted in Figure 6, which is in

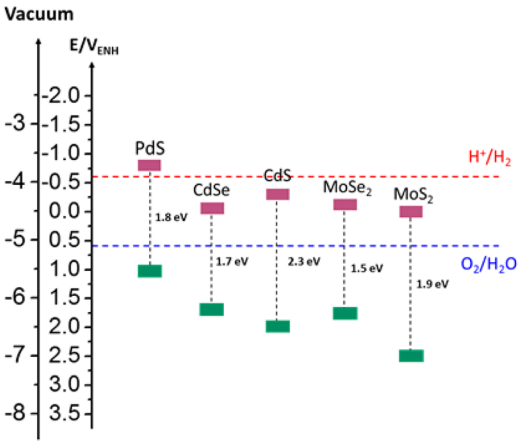


**Figure 6.** Conduction and valence band positions for several semiconducting metal sulfides in potential (V vs NHE) and energy (eV vs vacuum) scales. Redox potentials for the water-splitting half reactions at pH = 9.0 vs NHE are also included by the dashed lines. The water-splitting reaction is only thermodynamically favorable with PdS.

good agreement with that estimated from the work function of PdS previously reported ($\phi$ = 3,59 eV).[34] By using the energy band gap of PdS, the valence band energy position is also established. Other known metal selenides and sulfides are included in the figure for comparison purposes. Figure 6 also shows the energy levels of $H^+/H_2$ and $H_2O/O_2$ redox couples of reduction and oxidation of water at pH = 9 to elucidate if the photogenerated charge transfer from/to PdS is thermodynamically possible. From this figure is concluded that, since PdS conduction band edge is more negative than $H_2O/H_2$ redox potential, it may display photocatalytic activity for $H_2$ production. This activity will be demonstrated in the following section.

**Hydrogen Evolution.** It is indispensable to check the evolution of $H_2$ because it is not always assured that a high


dx.doi.org/10.1021/am5061504 | ACS Appl. Mater. Interfaces 2014, 6, 20544–20549

photocurrent value means high energy conversion efficiency. With this aim, a mass spectrometer coupled to the PEC has been used. Figure 7 shows the hydrogen generation rates at

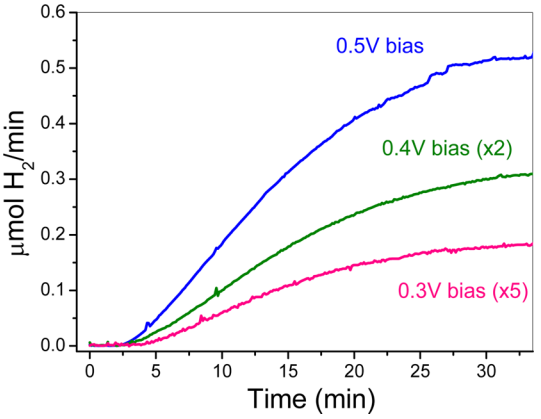


**Figure 7.** Time evolution of the rate of hydrogen production at different bias potentials.

different bias potentials. As it can be seen, at 0.5 V (Ag/AgCl), a stationary flux of 0.5 $\mu$mol $H_2$/min, approximately, is reached under illumination (in figure measures of bias potentials 0.3 V and 0.4 have been multiplied to observe all together, real flows in these cases can be observed in the Supporting Information). In Table 2, the rate of $H_2$ at different bias potentials can be

**Table 2. Hydrogen Evolution Rates, Photogenerated Hydrogen and Photoconversion Efficiency at Different Bias Potentials**

| bias potential (V) | $H_2$ rate ($\mu$mol$H_2$/min) | total $H_2$ in 30 min ($\mu$mol$H_2$) | photoconversion efficiency $\eta$ (%), eq 1 |
|---|---|---|---|
| 0.3 | 0.04 ± 0.05 | 2.2 ± 0.2 | 1.7 ± 0.2 |
| 0.4 | 0.16 ± 0.05 | 7.1 ± 0.2 | 2.7 ± 0.2 |
| 0.5 | 0.55 ± 0.05 | 23.2 ± 0.2 | 8.5 ± 0.2 |

observed. It is worthwhile to note that bare Ti substrates, previously investigated, did not show hydrogen evolution activity at all.

The PEC water splitting reaction utilizes light energy to drive thermodynamically uphill conversion of water to its constituents, hydrogen and oxygen. The whole reaction, as mentioned before, is assisted by a small applied voltage of 0.3 V, rather lower than those reported before with other semiconducting materials.[35] Gas flux in Figure 7 was measured with the mass spectrometer during the experiment. Table 2 resumes the photogeneration of hydrogen rates, total amount of hydrogen generated during 30 min and the photoconversion efficiency estimated at different $V_b$ by means of eq 1. Here, it is worthwhile to mention that the photoconversion efficiency is estimated using the illumination power density from the halogen lamp, reaching the photoanode surface and this light source has a different spectral response than the solar simulator. Therefore, this fact should be taken into account when these values are compared with the most of reported.

Hydrogen generation rates are comparable to those recently reported, obtained with structures formed by Cd chalcogenides (CdS, CdSe) quantum dots on ZnO nanowires, at similar bias potentials under solar AM1.5 illumination.[18] The total amount of hydrogen photogenerated during 30 min is higher than that estimated from the $H_2$ evolution rate by evolution time, hinting that the $H_2$ diffusion through the electrolyte to reach the mass spectrometer probe is a limiting rate step.

## CONCLUSIONS

PdS nanocorals has been synthesized and used as photoanodes in a PEC. The flat band potential of PdS in aqueous solutions is −0.65 ± 0.05 V (NHE), obtained from electrochemical impedance measurements under dark conditions, by using the Mott−Schottky plot.

An energy band levels scheme of the interface PdS/electrolyte is described that supports the feasibility to use PdS as photoanodes in photoelectrochemical systems to generate hydrogen is demonstrated.

Hydrogen is evolved in the counter electrode of a PEC with PdS as the photoanode under illuminations of 270 ± 20 mW/cm$^2$ at external bias potentials equal or higher than 0.3 V. The evolution rate and the amount of hydrogen photogenerated during 30 min, at different bias potentials, are quantified. The hydrogen evolution rates are comparable with those obtained using photoanodes based in more complex fabricated materials.

## ASSOCIATED CONTENT

### Supporting Information

Hydrogen evolution ratios at different bias potentials, calibration curve of mass spectrometer and characterization by X-ray before and after hydrogen generation measures. This material is available free of charge via the Internet at http://pubs.acs.org.

## AUTHOR INFORMATION

### Corresponding Author

*I. J. Ferrer. E-mail: isabel.j.ferrer@uam.es.

### Notes

The authors declare no competing financial interest.

## ACKNOWLEDGMENTS

The authors thank Dr. J. F. Fernández for his help with the Mass Spectrometry use and to Mr. J. Sousa and Mr. E. Delgado, from Nanotec Center, for the AFM measures. Technical support from Mr. F. Moreno and Financial support from MINECO (MAT2011-22780) are also acknowledged.

## ABBREVIATIONS

AFM = atomic force microscopy
EDX = energy dispersive X-ray spectroscopy
EIS = electrochemical impedance spectroscopy
FEG-SEM = field emission gun-scanning electron microscopy
PEC = photoelectrochemical cell
SEM = scanning electron microscopy
XRD = X-ray diffraction

## REFERENCES

(1) Bak, T.; Nowotny, J.; Rekas, M.; Sorrell, C. C. Photo-Electrochemical Hydrogen Generation from Water Using Solar Energy. Materials-Related Aspects. *Int. J. Hydrogen Energy* **2002**, *27*, 991−1022.

(2) Bard, A. J.; Whitesides, G. M.; Zare, R. N.; McLafferty, F. W. Holy Grails of Chemistry. *Acc. Chem. Res.* **1995**, *28*, 91−91.

(3) Fujishima, A.; Honda, K. Electrochemical Photolysis of Water at a Semiconductor Electrode. *Nature* **1972**, *238*, 37−38.

(4) Minggu, L. J.; Wan Daud, W. R.; Kassim, M. B. An Overview of Photocells and Photoreactors for Photoelectrochemical Water Splitting. *Int. J. Hydrogen Energy* **2010**, *35*, 5233−5244.
(5) Chen, X.; Shen, S.; Guo, L.; Mao, S. S. Semiconductor-based Photocatalytic Hydrogen Generation. *Chem. Rev.* **2010**, *110*, 6503−6570.
(6) Kalyanasundaram, K.; Borgarello, E.; Duonghong, D.; Grätzel, M. Cleavage of Water by Visible-Light Irradiation of Colloidal CdS Solutions; Inhibition of Photocorrosion by $RuO_2$. *Angew. Chem., Int. Ed. Engl.* **1981**, *20*, 987−988.
(7) Rajeshwar, K.; Licht, S.; McConnell, R. *Solar Hydrogen Generation: Toward a Renewable Energy Future*, 2008 ed.; Springer: New York, 2008.
(8) Licht, S.; Ghosh, S.; Tributsch, H.; Fiechter, S. High Efficiency Solar Energy Water Splitting to Generate Hydrogen Fuel: Probing $RuS_2$ Enhancement of Multiple Band Electrolysis. *Sol. Energy Mater. Sol. Cells* **2002**, *70*, 471−480.
(9) Sun, Y.; Liu, C.; Grauer, D. C.; Yano, J.; Long, J. R.; Yang, P.; Chang, C. J. Electrodeposited Cobalt-Sulfide Catalyst for Electrochemical and Photoelectrochemical Hydrogen Generation from Water. *J. Am. Chem. Soc.* **2013**, *135*, 17699−17702.
(10) Ferrer, I. J.; Díaz-Chao, P.; Pascual, A.; Sánchez, C. An Investigation on Palladium Sulphide (PdS) Thin Films as a Photovoltaic Material. *Thin Solid Films* **2007**, *515*, 5783−5786.
(11) Malik, M. A.; O'Brien, P.; Revaprasadu, N. Synthesis of TOPO-Capped PtS and PdS Nanoparticles from [Pt(S2CNMe(Hex))2] and [Pd(S2CNMe(Hex))2]. *J. Mater. Chem.* **2002**, *12*, 92−97.
(12) Folmer, J. C. W.; Turner, J. A.; Parkinson, B. A. Photoelectrochemical Characterization of Several Semiconducting Compounds of Palladium with Sulfur and/or Phosphorus. *J. Solid State Chem.* **1987**, *68*, 28−37.
(13) Maciá, M. D.; Díaz-Chao, P.; Clamagirand, J. M.; Ares, J. R.; Ferrer, I. J.; Sánchez, C. Photoelectrochemical Properties of Palladium Sulfide (PdS). In *Proceedings of the First International Conference on Materials for Energy, Extended Abstracts - Book A*; DECHEMA: Frankfurt, 2010; pp 526−528.
(14) Yan, H.; Yang, J.; Ma, G.; Wu, G.; Zong, X.; Lei, Z.; Shi, J.; Li, C. Visible-Light-Driven Hydrogen Production with Extremely High Quantum Efficiency on Pt−PdS/CdS Photocatalyst. *J. Catal.* **2009**, *266*, 165−168.
(15) Yang, J.; Yan, H.; Wang, X.; Wen, F.; Wang, Z.; Fan, D.; Shi, J.; Li, C. Roles of Cocatalysts in Pt−PdS/CdS with Exceptionally High Quantum Efficiency for Photocatalytic Hydrogen Production. *J. Catal.* **2012**, *290*, 151−157.
(16) Zhang, X.; Sun, Y.; Cui, X.; Jiang, Z. A Green and Facile Synthesis of $TiO_2$/graphene Nanocomposites and Their Photocatalytic Activity for Hydrogen Evolution. *Int. J. Hydrogen Energy* **2012**, *37*, 811−815.
(17) Wang, Q.; Li, J.; An, N.; Bai, Y.; Lu, X.; Li, J.; Ma, H.; Wang, R.; Wang, F.; Lei, Z.; Shangguan, W. Preparation of a Novel Recyclable Cocatalyst Wool−Pd for Enhancement of Photocatalytic $H_2$ Evolution on CdS. *Int. J. Hydrogen Energy* **2013**, *38*, 10761−10767.
(18) Seol, M.; Jang, J.-W.; Cho, S.; Lee, J. S.; Yong, K. Highly Efficient and Stable Cadmium Chalcogenide Quantum Dot/ZnO Nanowires for Photoelectrochemical Hydrogen Generation. *Chem. Mater.* **2013**, *25*, 184−189.
(19) Cullity, B. D. *Elements Of X Ray Diffraction*; Addison-Wesley Publishing Company, Inc.: Reading, MA, 1956.
(20) Orazem, M. E. *Electrochemical Impedance Spectroscopy*; John Wiley & Sons: New York, 2008.
(21) Li, H.; Cheng, C.; Li, X.; Liu, J.; Guan, C.; Tay, Y. Y.; Fan, H. J. Composition-Graded ZnxCd1−xSe@ZnO Core−Shell Nanowire Array Electrodes for Photoelectrochemical Hydrogen Generation. *J. Phys. Chem. C* **2012**, *116*, 3802−3807.
(22) Bard, A. J.; Faulkner, L. R.. *Electrochemical Methods: Fundamentals and Applications*; John Wiley &Sons: New York, 1980.
(23) Chang, K.; Mei, Z.; Wang, T.; Kang, Q.; Ouyang, S.; Ye, J. $MoS_2$/Graphene Cocatalyst for Efficient Photocatalytic $H_2$ Evolution under Visible Light Irradiation. *ACS Nano* **2014**, *8*, 7078−7087.
(24) Pareek, A.; Purbia, R.; Paik, P.; Hebalkar, N. Y.; Kim, H. G.; Borse, P. H. Stabilizing Effect in Nano-Titania Functionalized CdS Photoanode for Sustained Hydrogen Generation. *Int. J. Hydrogen Energy* **2014**, *39*, 4170−4180.
(25) Grimes, C.; Varghese, O.; Ranjan, S. *Light, Water, Hydrogen: The Solar Generation of Hydrogen by Water Photoelectrolysis*; 2008 ed.; Springer: New York, 2007.
(26) Power Diffraction File Alphabetical Index, ICDD, International Center for Diffraction Data, Swarthmore, PA (JCPDS-ICDD 44-1288, JCPDS-ICDD 46-1043, JCPDS-ICDD 78-0206).
(27) Diaz-Chao, P.; Ferrer, I. J.; Ares, J. R.; Sanchez, C. Cubic Pd16S7 as a Precursor Phase in the Formation of Tetragonal PdS by Sulfuration of Pd Thin Films. *J. Phys. Chem. C* **2009**, *113*, 5329−5335.
(28) Horcas, I.; Fernández, R.; Gómez-Rodríguez, J. M.; Colchero, J.; Gómez-Herrero, J.; Baro, A. M. WSXM: A Software for Scanning Probe Microscopy and a Tool for Nanotechnology. *Rev. Sci. Instrum.* **2007**, *78*, 013705.
(29) Bard, A. J. Photoelectrochemistry. *Science* **1980**, *207*, 139−144.
(30) Finklea, H. O. Photoelectrochemistry: Introductory Concepts. *J. Chem. Educ.* **1983**, *60*, 325.
(31) Walter, M. G.; Warren, E. L.; McKone, J. R.; Boettcher, S. W.; Mi, Q.; Santori, E. A.; Lewis, N. S. Solar Water Splitting Cells. *Chem. Rev.* **2010**, *110*, 6446−6473.
(32) Ni, M.; Leung, M. K. H.; Leung, D. Y. C.; Sumathy, K. A Review and Recent Developments in Photocatalytic Water-Splitting Using for Hydrogen Production. *Renewable Sustainable Energy Rev.* **2007**, *11*, 401−425.
(33) Butler, M. A.; Ginley, D. S. Principles of Photoelectrochemical, Solar Energy Conversion. *J. Mater. Sci.* **1980**, *15*, 1−19.
(34) Haque, C. A.; Fritz, J. H. Work Function Changes on Contact Materials. *IEEE Trans. Parts, Hybrids, Packag.* **1974**, *10*, 27−31.
(35) Ng, C.; Ng, Y. H.; Iwase, A.; Amal, R. Influence of Annealing Temperature of WO3 in Photoelectrochemical Conversion and Energy Storage for Water Splitting. *ACS Appl. Mater. Interfaces* **2013**, *5*, 5269−5275.